

**VISIBLE-NEAR INFRARED (VIS-NIR)
SPECTROSCOPY FOR QUANTIFICATION OF
HELA AND DU145 CELLS**

SUHAINAH BINTI SUDIK

UNIVERSITI SAINS MALAYSIA

2020

**VISIBLE–NEAR INFRARED (VIS-NIR)
SPECTROSCOPY FOR QUANTIFICATION OF
HELA AND DU145 CELLS**

by

SUHAINAH BINTI SUDIK

**Thesis submitted in fulfilment of the requirements
for the degree of
Doctor of Philosophy**

November 2020

ACKNOWLEDGEMENT

All praise to be to Allah, the Almighty, and the Benevolent for His blessings and guidance for giving me the inspiration, ability, and strength to be able to accomplish this research. I would like to express my gratitude to all who have been involved in this study and aided in making it successful. I offer my special gratitude to my parents for the persistent support given and all the advice that derived me from the accomplishment of this research. I would not have done it without my family's persistent support and encouragement. I would like to express my deepest gratitude to my supervisor, Dr. Ahmad Fairuz Bin Omar, for providing the opportunity of this study with the project given and his continuous guidance, endless support, and all the knowledge that has inspired me throughout this study. I also would like to thank profusely my co-supervisor, Associate Professor Dr. Md Azman Seeni Mohamed for appropriate advice and knowledge who willing to assist me during my project at Integrative Medicine Cluster, Advanced Medical and Dental Institute (AMDI), Universiti Sains Malaysia (USM). It has been a great pleasure and honour to have them as my supervisors. I would like to extend my appreciation towards Mr. Mohd Hafiz Mail for the advice and guidance on my lab work during the samples' preparation in AMDI. My special thanks to Mr. Mohtar Sabdin who is a lab assistant in the School of Physics that has assisted me in the utilisation of facilities at the engineering physics laboratory. I would like to sincerely thank Mr. Firdaus who is a lab assistant in the AMDI laboratory that helped me a lot. Last but not least, thanks to all my friends who were with me and support me through thick and thin. This journey would not have been possible without everyone's support and guidance. This study was partly

supported by Universiti Sains Malaysia - Bridging Grant (Grant No. 304 / PFIZIK / 6316532).

TABLE OF CONTENTS

ACKNOWLEDGEMENT	ii
TABLE OF CONTENTS	iv
LIST OF TABLES	viii
LIST OF FIGURES	xi
LIST OF SYMBOLS	xviii
LIST OF ABBREVIATIONS	xix
LIST OF APPENDICES	xxi
ABSTRAK	xxii
ABSTRACT	xxiv
CHAPTER 1 INTRODUCTION	1
1.1 Research Background.....	1
1.2 The Fundamental of Cancer	3
1.2.1 Cervical Cancer	4
1.2.2 Prostate Cancer.....	7
1.3 Skin Fibroblasts.....	10
1.4 Cell Culture and Cell Culture Media.....	12
1.5 The Fundamental of Optical Spectroscopy	15
1.5.1 Overview of VIS-NIR Spectroscopy.....	16
1.5.2 The Interaction of Light with Matter.....	18
1.5.3 Absorbance and Concentration: The Beer-Lambert Law	18
1.5.4 Optical Spectroscopy in Cancer Diagnosis	19
1.6 Problem Statement of the Research.....	21
1.6.1 Social Concern and Addressing Sustainable Development Goals.....	21
1.6.2 Research Gaps in Cancer Detection	22

1.7	Aim and Objectives	24
1.7.1	Aim.....	24
1.7.2	Objectives of Research.....	25
1.8	Significance of the Research	25
1.9	Scope of the Research	26
1.10	Arrangement of Chapters	28
CHAPTER 2 LITERATURE REVIEW.....		31
2.1	Introduction	31
2.2	Principle of Spectroscopy for Cancer Diagnosis.....	32
2.3	Diagnostic Instruments and Techniques for Cervical and Prostate Cancer ...	37
2.3.1	Diagnostic for Cervical Cancer	38
2.3.2	Diagnostic for Prostate Cancer.....	42
2.4	Spectroscopic Approaches in Cancer Diagnostic and Spectroscopic Application in Cervical and Prostate Cancer	47
2.4.1	Spectroscopic Application in Cervical and Prostate Cancer.....	52
2.4.2	Role and Impact of UV-VIS-NIR Spectroscopy in Cervical and Prostate Cancer Diagnosis.....	56
2.5	Morphological Differences and Optical Properties of Normal and Cancerous Cells.....	62
2.5.1	Morphological Differences	67
2.5.2	Optical Properties	69
CHAPTER 3 METHODOLOGY.....		72
3.1	Introduction	72
3.2	Cell Types and Specifications	72
3.2.1	L929 Cells	73
3.2.2	DU145 Cells.....	73
3.2.3	HeLa Cells.....	74
3.3	Cell Culture Media and Equipment.....	74

3.4	Cell Culture Technique	77
3.4.1	Sample Preparation and Basic Precaution.....	77
3.4.2	Thawing Frozen Cells	80
3.4.3	Subculture.....	81
3.4.4	Cell Counting	83
3.4.5	Cell Seeding	87
3.4.6	Cryopreservation	90
3.5	Cell Morphology	91
3.6	Optical Spectroscopic Instrumentation	92
3.6.1	VIS-NIR Spectrometer	92
3.6.2	Light Source and Probe	94
3.6.3	SpectraSuite Software	95
3.7	Experimental Setup	97
3.8	Spectral Quantitative Analysis	100
3.8.1	Simple Linear Regression	100
3.8.2	Multiple Linear Regressions	102
3.8.3	The Selection of Wavelength	104
3.8.4	Spectral Signature	105
CHAPTER 4	RESULTS AND DISCUSSIONS	107
4.1	Introduction	107
4.2	Visible Absorbance Measurement with Phenol Red Media.....	107
4.3	VIS-NIR Absorbance Measurement of Normal and Cancerous Cells in Cell Culture Media with Phenol Red	110
4.4	Morphological Observation of Cell Culture Media with Phenol Red.....	124
4.5	VIS-NIR Spectral Signatures of Normal and Cancerous Cells in Cell Culture Media with Phenol Red through Regression Analysis.....	130
4.5.1	Coefficient of Determination, R^2	131
4.5.2	Slope (Responsivity)	134

4.6	VIS-NIR Quantitative Analysis of Normal and Cancerous Cells in Cell Culture Medium with Phenol Red.....	137
4.7	VIS-NIR Absorbance Measurement of Normal and Cancerous Cells in Cell Culture Media without Phenol Red	142
4.8	Morphological Observation of Cell Culture Media without Phenol Red.....	151
4.9	VIS-NIR Spectral Signatures of Normal and Cancerous Cells in Cell Culture Media without Phenol Red through Regression Analysis.....	157
4.9.1	Coefficient of Determination, R^2	157
4.9.2	Slope (Responsivity)	160
4.10	VIS-NIR Quantitative Analysis of Normal and Cancerous Cells in Cell Culture without Phenol Red	162
4.11	Producibility of Cells' Quantitative Analysis between Culture Cell Lines with and without Phenol Red	168
4.12	Summary	176
CHAPTER 5 CONCLUSION AND FUTURE RECOMMENDATIONS....		181
5.1	Conclusion.....	181
5.2	Recommendations for Future Research	183
REFERENCES.....		185
APPENDICES		
LIST OF PUBLICATIONS		

LIST OF TABLES

	Page
Table 1.1 Differentiate between mouse skin and human skin (Pasparakis et al., 2014) (Lawlor & Kaur, 2015).	11
Table 2.1 Summary of optical spectroscopic techniques for the study of biological cells (Wax et al., 2012).	35
Table 2.2 Sample types for cancer detection by FTIR with spectral analyses (Kumari, Kaur, & Bhattacharyya, 2018).....	48
Table 2.3 Summary of in vivo Raman spectroscopy for oncology applications (McGregorH et al., 2016).	49
Table 2.4 Comparison between Raman spectroscopy and FTIR (Kast et al., 2014).	50
Table 2.5 Various medical applications of IR radiation for different cells and tissues (Tsai & Hamblin, 2017).	50
Table 2.6 Characteristics of various optical spectroscopy techniques in diagnosis (Wan, Wang, & Zhang, 2017).	58
Table 2.7 Morphological differences in normal cells and cancer cells (LaMorte, 2016) (Kumar, 2015).	67
Table 3.1 Specifications of L929 cells (ATCC ^a , 2018).	73
Table 3.2 Specifications of DU145 cells (ATCC ^b , 2018).....	74
Table 3.3 Specifications of HeLa cells (ATCC, 2019).	74
Table 3.4 Cells concentration was calculated for L929, HeLa, and DU145 cells with phenol red.	86
Table 3.5 Cells concentration was calculated for L929, HeLa, and DU145 cells without phenol red.	86
Table 3.6 Cells concentration and volume of medium for L929, HeLa, and DU145 cells with phenol red.	88

Table 3.7	Cells concentration and volume of medium for L929, HeLa, and DU145 cells without phenol red.	88
Table 3.8	Different numbers of cells in each sample for spectroscopic measurement with phenol red.	88
Table 3.9	Different numbers of cells in each sample for spectroscopic measurement without phenol red.	89
Table 4.1	Cell morphology with 10 times magnification for L929, HeLa, and DU145 cells for 50 000 cells, 75 000 cells, and 100 000 cells.	127
Table 4.2	Cell morphology with 10 times magnification for L929, HeLa, and DU145 cells for 125 000 cells, 150 000 cells, and 175 000 cells. ...	128
Table 4.3	Cell morphology with 10 times magnification for L929, HeLa, and DU145 cells for 200 000 cells, 225 000 cells, 250 000 cells, and 275 000 cells.	129
Table 4.4	Calibration results from MLR using wavelengths for L929 cells.	137
Table 4.5	Calibration results from MLR using wavelengths for HeLa cells. ...	139
Table 4.6	Calibration results from MLR using wavelengths DU145 cells.	140
Table 4.7	Cell morphology with 10 times magnification of L929, HeLa, and DU145 cells for 50 000 cells, 75 000 cells, and 100 000 cells in cell culture media without phenol red.	154
Table 4.8	Cell morphology with 10 times magnification of L929, HeLa, and DU145 cells for 125 000 cells, 150 000 cells, and 175 000 cells in cell culture media without phenol red.	155
Table 4.9	Cell morphology with 10 times magnification of L929, HeLa, and DU145 cells for 200 000 cells, 225 000 cells, 250 000 cells, and 275 000 cells in cell culture media without phenol red.	156
Table 4.10	Calibration results from MLR using wavelengths for L929 cells in cell culture media without phenol red.	163
Table 4.11	Calibration results from MLR using wavelengths for HeLa cells in cell culture media without phenol red.	164

Table 4.12	Calibration results from MLR using wavelengths of DU145 cells in cell culture media without phenol red.....	166
Table 4.13	Summary of results obtained from quantitative analysis of cell media with phenol red.....	180
Table 4.14	Summary of results obtained from the quantitative analysis of cell media without phenol red.....	180

LIST OF FIGURES

	Page
Figure 1.1	Abnormal cell expansion (Nejmadi, 2010)4
Figure 1.2	Normal cell and different stages of cervical cancer cells (Schilling, 2018).6
Figure 1.3	Multiphoton fluorescence image of HeLa cells with cytoskeletal microtubules (magenta) and DNA (cyan) using Nikon RTS2000MP custom laser scanning microscope (Image by National Institutes of Health (NIH)).6
Figure 1.4	Illustration of normal prostate versus a prostate with a tumor prostate cancer. (Mandal, 2018).9
Figure 1.5	Morphology of the DU145 cell lines in culture with 100x magnification. DU145 cells show a more mesenchymal morphology that is long and spindle-shaped (Carey et al., 2009).9
Figure 1.6	Different techniques used for primary culture (Jha, 2015). 13
Figure 1.7	Animal cell culture to produce a cell line (Khanal, 2017). 14
Figure 1.8	Basic categories of morphology cells in cell culture based on shape and appearance (A) fibroblastic, (B) epithelial, and (C) lymphoblast. The images were obtained using 20x magnification (Invitrogen, 2010). 14
Figure 1.9	The electromagnetic spectrum describes the various types of electromagnetic energy based on the wavelength (Protherm, 2005). 17
Figure 1.10	Flow chart of research analysis.28
Figure 2.1	Light passing through an optical fiber (Ocean Optics, 2013).33
Figure 2.2	Light interacts with matter includes reflection, absorption, transmittance, scatter, fluorescence (Spectroscopy, 2015).34

Figure 3.1	Two types of DMEM media (a) Medium with phenol red and (b) Medium without phenol red.	75
Figure 3.2	Comparison of contaminated compared to normal cell culture in the flask.	79
Figure 3.3	Normal (A and C) and contaminated (Band D) cell culture image with 10x magnification (picture A and picture B) and 20x magnification (picture C and picture D).	79
Figure 3.4	Preparation of cell culture experiment in biosafety cabinet.	80
Figure 3.5	Process of thawing frozen cell; (a) Cryovial was thawed in a water bath; (b) The cell was mixed of vial content and media; (c) The cell was centrifuged; (d) The supernatant was discarded and was transferred into the flask with new media and remaining cell pellet; (e) The cell was placed in the incubator.	81
Figure 3.6	Summary of subculture process.	83
Figure 3.7	Process of haemocytometer counting. (a) Cells were pipetted into microtube; (b) Trypan blue dye was added into microtube; (c) The mixture was placed onto a haemocytometer chamber; (d) Cells were counted under an inverted microscope.	85
Figure 3.8	Counting cells on the haemocytometer (Fuentes, 2013).	85
Figure 3.9	Cells seeding in 6 well plates.	87
Figure 3.10	(a) Cyrovial in the box was placed in (b) freezer, - 20 ⁰ C to freeze the cells.	91
Figure 3.11	Inverted microscopes and its parts.	92
Figure 3.12	(a) QE65000 Spectrometer (b) Components inside spectrometer (Ocean Optics, 2009).	93
Figure 3.13	(a) Halogen lamp (b) Main components of a halogen lamp.	94
Figure 3.14	(a) Optical fiber (b) Component layer of fiber.	94
Figure 3.15	SpectraSuite Software panel display.	96
Figure 3.16	Illustration of operation inside the measurement chamber.	99

Figure 3.17	Illustration of typical absorbance spectroscopy measurements conducted on control samples.....	100
Figure 4.1	Absorbance spectra of control sample for different pH levels and the color changes of phenol red.	109
Figure 4.2	Linear relationship at 557nm between absorbance and pH of phenol red.....	109
Figure 4.3	Graph of the coefficient determination R^2 versus wavelength (nm) for the control sample in the visible region.....	109
Figure 4.4	Absorbance spectra for L929, HeLa, and DU145 cultured cell lines with 50 000 number of cells.....	111
Figure 4.5	Absorbance spectra for L929, HeLa, and DU145 cultured cell lines with 75 000 number of cells.....	112
Figure 4.6	Absorbance spectra for L929, HeLa, and DU145 cultured cell lines with 100 000 number of cells.....	113
Figure 4.7	Absorbance spectra for L929, HeLa, and DU145 cultured cell lines with 125 000 number of cells.....	113
Figure 4.8	Absorbance spectra for L929, HeLa, and DU145 cultured cell lines with 150 000 number of cells.....	114
Figure 4.9	Absorbance spectra for L929, HeLa, and DU145 cultured cell lines with 175 000 number of cells.....	115
Figure 4.10	Absorbance spectra for L929, HeLa, and DU145 cultured cell lines with 200 000 number of cells.....	116
Figure 4.11	Absorbance spectra for L929, HeLa, and DU145 cultured cell lines with 225 000 number of cells.....	117
Figure 4.12	Absorbance spectra for L929, HeLa, and DU145 cultured cell lines with 250 000 number of cells.....	117
Figure 4.13	Absorbance spectra for L929, HeLa and DU145 cultured cell lines with 275 000 number of cells.....	118
Figure 4.14	Absorbance spectra at different pH levels (Held, 2018).....	120

Figure 4.15	The absorbance spectrum of the different numbers of (a) L929, (b) HeLa, and (c) DU145 cells. Absorbance versus the number of cells (d) 557 nm and (e) 960 nm for cell media with phenol red.	124
Figure 4.16	Microscopic images of (a) L929, (b) HeLa, and (c) DU145 cells with 20 times magnification to enhance the visual observation of the cell morphology with phenol red in term of size of each cell. ...	130
Figure 4.17	Coefficient of determination, R^2 , and slope for absorbance spectra of L929 cells at 557 nm.....	131
Figure 4.18	Coefficient of determination, R^2 generated using linear regression in the quantitative measurement of cells between 400 nm and 1100 nm for L929, HeLa, and DU145 cells in (a) Well-A (b) Well-B (c) Well-C.....	133
Figure 4.19	Coefficient of determination, R^2 generated using linear regression in the quantitative measurement of cells between 400 nm and 1100 nm for L929, HeLa, and DU145 cells.....	134
Figure 4.20	Responsivity generated using linear regression in the quantitative measurement of cells between 400 nm and 1100 nm for L929, HeLa, and DU145 cells in (a) Well-A (b) Well-B (c) Well-C.....	136
Figure 4.21	Responsivity generated using linear regression in the quantitative measurement of cells between 400 nm and 1100 nm for L929, HeLa, and DU145.	136
Figure 4.22	Correlation graph between the actual number of cells and the number of cells computed (calculated) through the spectroscopic algorithm for quantitative measurement of L929 cells.	138
Figure 4.23	Correlation graph between the actual number of cells and the number of cells computed (calculated) through the spectroscopic algorithm for quantitative measurement of HeLa cells.....	140
Figure 4.24	Correlation graph between the actual number of cells and the number of cells computed (calculated) through the spectroscopic algorithm for quantitative measurement of DU145 cells.....	141

Figure 4.25	Absorbance spectra for L929, HeLa, and DU145 cultured cell lines with 50 000 number of cells in cell culture media without phenol red.....	142
Figure 4.26	Absorbance spectra for L929, HeLa, and DU145 cultured cell lines with 75000 number of cells in cell culture media without phenol red.....	143
Figure 4.27	Absorbance spectra for L929, HeLa, and DU145 cultured cell lines with 100 000 number of cells in cell culture media without phenol red.....	144
Figure 4.28	Absorbance spectra for L929, HeLa, and DU145 cultured cell lines with 125 000 number of cells in cell culture media without phenol red.....	144
Figure 4.29	Absorbance spectra for L929, HeLa, and DU145 cultured cell lines with 150 000 number of cells in cell culture media without phenol red.....	145
Figure 4.30	Absorbance spectra for L929, HeLa, and DU145 cultured cell lines with 175 000 number of cells in cell culture media without phenol red.....	146
Figure 4.31	Absorbance spectra for L929, HeLa, and DU145 cultured cell lines with 200 000 number of cells in cell culture media without phenol red.....	146
Figure 4.32	Absorbance spectra for L929, HeLa, and DU145 cultured cell lines with 225 000 number of cells in cell culture media without phenol red.....	147
Figure 4.33	Absorbance spectra for L929, HeLa, and DU145 cultured cell lines with 250 000 number of cells in cell culture media without phenol red.....	147
Figure 4.34	Absorbance spectra for L929, HeLa, and DU145 cultured cell lines with 275 000 number of cells in cell culture media without phenol red.....	148

Figure 4.35	The absorbance spectrum of different numbers of (a) L929, (b) HeLa, and (c) DU145 cells. Absorbance versus the number of cells for (d) 557 nm and (e) 960 nm for cell media without phenol red... 151
Figure 4.36	Microscopic images of (a) L929, (b) HeLa, and (c) DU145 cells with 20 times magnification to enhance the visual observation of the cell morphology without phenol red in term of size of each cell. 157
Figure 4.37	Coefficient of determination, R^2 for cell culture media without phenol red generated using linear regression in the quantitative measurement of cells between 400 nm and 1100 nm for L929, HeLa, and DU145 cells in (a) Well-A (b) Well-B (c) Well-C..... 159
Figure 4.38	Coefficient of determination, R^2 for cell culture media without phenol red generated using linear regression in the quantitative measurement of cells between 400 nm and 1100 nm for L929, HeLa, and DU145 cells..... 160
Figure 4.39	Responsivity for cell culture media without phenol red generated using linear regression in the quantitative measurement of cells between 400 nm and 1100 nm for L929, HeLa, and DU145 cells in (a) Well-A (b) Well-B (c) Well-C..... 162
Figure 4.40	Responsivity for cell culture media without phenol red generated using linear regression in the quantitative measurement of cells between 400 nm and 1100 nm for L929, HeLa, and DU145 cells... 162
Figure 4.41	Correlation graph between the actual number of cells and the number of cells computed (calculated) through the spectroscopic algorithm for quantitative measurement of L929 cells in cell culture media without phenol red..... 164
Figure 4.42	Correlation graph between the actual number of cells and the number of cells computed (calculated) through the spectroscopic algorithm for quantitative measurement of HeLa cells in cell culture media without phenol red..... 165

Figure 4.43	Correlation graph between the actual number of cells and the number of cells computed (calculated) through the spectroscopic algorithm for quantitative measurement of DU145 cells in cell culture media without phenol red.....	167
Figure 4.44	Absorbance distribution between cell media with and without phenol red for L929 cells with numbers of cells (a) 100 000 cells and (b) 225 000 cells.....	169
Figure 4.45	Absorbance distribution between cell media with and without phenol red for HeLa cells with numbers of cells (a) 100 000 cells and (b) 225 000 cells.....	170
Figure 4.46	Absorbance distribution between cell media with and without phenol red for DU145 cells with numbers of cells (a) 100 000 cells and (b) 225 000 cells.....	170
Figure 4.47	Absorbance spectra by using subtraction of absorbance cell media with and without phenol red for (a) L929 cells (b) HeLa cells, and (c) DU145 cells	172
Figure 4.48	Predicted versus the actual number of cells for (a) L929 cells, (b) HeLa cells, and (c) DU145 cells by using calibration equation from cells with phenol red media and applied it to cells without phenol red media.....	174
Figure 4.49	The prediction graph of the number of cells for (a) L929 cells, (b) HeLa cells, and (c) DU145 cells with MLR results from the combinations of absorbance data for both cells media with and without phenol red.....	176
Figure 4.50	Absorbance spectra of the control sample (media with phenol red only) for different pH levels and cell media with phenol red for 100 000 L929, HeLa, and DU145 cells.....	177

LIST OF SYMBOLS

%	Percent
μL	Microliter
$^{\circ}\text{C}$	Degree Celsius
CH_3	Methyl group
cm	Centimeter
CO_2	Carbon dioxide
Df	Dilution factors
EtOH	Ethanol
Hf	Haemocytometer factor
I	Intensity
ml	Milliliter
mm	Millimeter
mm^2	Square millimeter
ms	milliseconds
N_2	Liquid nitrogen
NaB	Sodium butyrate
nm	Nanometer
O-H	Oxygen-hydrogen
PO_2	Phosphate
R^2	Coefficient of Determination
rpm	Revolution per minute
V	Voltage
W	Watt
λ	wavelength
μm	Micrometer

LIST OF ABBREVIATIONS

A/D	Analog-to-digital
a/LCI	Angle-resolved low coherence interferometry
AMDI	Integrative Medicine Cluster, Advanced Medical and Dental Institute
ATTC	American Type Culture Collection
CARS	Coherent anti-Stokes Raman scattering
CCD	Charge-coupled device
CEA	Carcinoembryonic antigen
CT	Computed Tomography
DMEM	Dulbecco's Modified Eagle Medium
DMSO	Dimethyl sulfoxide
DNA	Deoxyribonucleic acid
DRE	Digital rectal examination
ECC	Endocervical curettage
EDTA	Ethylenediaminetetraacetic acid
ESR	Electron spin resonance spectroscopy
FAD	Flavin adenine dinucleotide
FBS	Fetal Bovine Serum
FDG	Fluorodeoxyglucose
fLCI	Fourier domain low-coherence interferometry
FTIR	Fourier-transform infrared spectroscopy
FTLS	Fourier transform light scattering
GI	Gastrointestinal
HDI	Human development index
HGPIN	High grade prostatic intraepithelial neoplasia
HPV	Human papillomavirus
H-SIL	Intra-epithelial lesions
ILC	Innate lymphoid cells
IO	Input-output
IPS	Institut Pengajian Siswazah
IR	Infrared
IRAM	Integrated Raman- and angular-scattering microscopy system

LBC	Liquid-based cytology
LGPIN	Low grade prostatic intraepithelial neoplasia
LSS	Light scattering spectroscopy
MEM	Minimum Essential Medium
MIR	Mid-infrared
MLR	Multiple linear regression
MRI	Magnetic Resonance Imaging
NA	Not available
NADH	Nicotinamide adenine dinucleotide
NIR	Near-Infrared
NMR	Nuclear magnetic resonance
PCA	Principal Component Analysis
PC-DFA	Principal component-discriminant function analysis
PET	Positron emission tomography
PIN	Prostatic intraepithelial neoplasia
PLS	Partial Least Squares
PPE	Personal protective equipment
PPV	Positive predictive value
PSA	Prostate-specific antigen
PWS	Partial wave spectroscopy
RMSE	Root Mean Square Error
SDS	Safety datasheet
SPA-LDA	Partial least squares discriminant analysis
SRS	Stimulated Raman scattering
TE	Thermoelectric
TRUS	Transrectal Ultrasound
US	Ultrasound
USB	Universal Serial Bus
USM	Universiti Sains Malaysia
UV	Ultraviolet
VIA	Visual inspection with acetic acid
VIS	Visible

LIST OF APPENDICES

Appendix A	Normalised coefficient of determination, R^2 , and responsivity (phenol red)
Appendix B	Normalised coefficient of determination, R^2 , and responsivity (without phenol red)

SPEKTROSKOPI SINAR NAMPAK DAN INFRAMERAH DEKAT (VIS-NIR) BAGI KUANTIFIKASI SEL HELA DAN DU145

ABSTRAK

Salah satu daripada penyebab utama kematian di seluruh dunia adalah penyakit kanser. Teknik diagnosis yang paling biasa digunakan untuk penyakit kanser adalah menggunakan sinaran mengion seperti teknik imbasan yang memerlukan sumber kewangan yang tinggi dan infrastruktur khusus yang mana menghadkan penggunaan kaedah ini. Manakala, spektroskopi optik ialah tiada sinaran mengion yang menunjukkan potensi besar sebagai alat tambahan untuk mengdiagnosis kanser, salah satunya ialah dengan mempamerkan keupayaan untuk menghasilkan pencirian spektroskopi khusus di antara tisu normal dan tisu kanser. Dalam kajian ini, pengukuran serapan sinar nampak dan inframerah dekat, VIS-NIR (400-1100 nm) spektroskopi untuk media dengan dan tiada fenol merah oleh kanser pangkal rahim (HeLa) dan kanser prostat (DU145) turunan sel digunakan melalui teknik kultur sel. Dalam penyelidikan awal, perubahan warna fenol merah daripada merah jambu terang ($\text{pH} = 8.1$) kepada merah jambu cerah ($\text{pH} = 7.62$) sangat berkaitan dengan pengasidan medium kultur sel pada sampel kawalan dengan responsiviti puncak pada 557 nm. Di kawasan sinar nampak dengan media fenol merah, nilai penyerapan puncak dengan bilangan sel yang berbeza adalah pada panjang gelombang daripada 556nm hingga 559nm dikenal pasti berkaitan dengan penyerapan warna dalam media. Walau bagaimanapun, spektrum serapan tidak menghasilkan sebarang puncak yang ketara yang memberikan maklumat mengenai warna di kawasan sinar nampak tanpa media fenol merah disebabkan sifat media yang digunakan dalam kultur sel adalah yang tidak berwarna. Panjang gelombang diantara 966 nm dan 985 nm telah dijumpai dan

dikenal pasti sangat berkaitan dengan penyerapan air di kawasan inframerah dekat. Nilai serapan sedikit meningkat untuk setiap kenaikan bilangan sel untuk semua turunan sel disebabkan oleh penyerapan cahaya oleh sel. Bentuk spektrum untuk sel yang dikaji telah dihitung daripada regresi linear (iaitu dihasilkan daripada hubungan di antara penyerapan daripada 400 hingga 1100 nm dan bilangan sel) parameter-parameter seperti algoritma spektroskopi, R^2 dan cerun (responsiviti). Pola pada bentuk spektrum untuk sel dengan ketara meningkatkan lagi pelbagai kecerian diantara sel-sel L929, HeLa and DU145. Analisis pelbagai regresi linear (MLR) digunakan bagi menghasilkan algoritma untuk kuantifikasi sel kanser dengan menggunakan Perisian Minitab 18. Kombinasi terbaik daripada beberapa panjang gelombang untuk setiap cell dapat dikenal pasti untuk menghasilkan algoritma spektroskopi dengan R^2 yang tinggi dan RMSE yang rendah. Ketepatan pengukuran terbaik dengan $R^2 = 99.89\%$, $R^2 = 99.68\%$ dan $R^2 = 99.63\%$ dihasilkan dengan RMSE = 3390 sel, RMSE = 5277 sel dan RMSE = 5647 sel untuk sel L929, DU145 dan HeLa masing-masing untuk media dengan fenol merah manakala media tanpa fenol merah untuk sel-sel L929, DU145 dan HeLa menghasilkan $R^2 = 99.94\%$, $R^2 = 99.91\%$ dan $R^2 = 99.44\%$ dengan RMSE = 1860 sel, RMSE = 2754 sel, dan RMSE = 6938 sel masing-masing. Pengukuran ketepatan yang tinggi oleh sel dengan pekali penentuan atas 0.99 dihasilkan daripada kuantitatif analisis untuk semua sel. Kajian ini telah membuktikan bahawa pelbagai spektroskopi serapan VIS-NIR dapat dilakukan untuk membezakan di antara sel normal dan sel kanser yang berpotensi sebagai biomarker spektroskopi kanser dan sebagai alat pengukuran kuantitatif sel.

VISIBLE–NEAR INFRARED (VIS-NIR) SPECTROSCOPY FOR QUANTIFICATION OF HELA AND DU145 CELLS

ABSTRACT

The most common diagnostic techniques for cancer include ionizing testing such as imaging techniques require significant financial resources and infrastructure, which limit access to these modalities. In contrast, optical spectroscopy is non-ionizing testing that has shown promising potential as additional tools for cancer diagnosis, one of it through exhibiting the ability to display distinctive spectral characteristics between normal and cancerous tissues. In this study, the visible and near-infrared, VIS–NIR (400-1100 nm) absorbance spectroscopy measurement with and without phenol red cultured media of cervical cancer (HeLa) and prostate cancer (DU145) cell lines was used through cell culturing technique. In the preliminary investigation, the color changes of phenol red from bright pink (pH = 8.1) to light pink (pH = 7.62) were highly correlated to the acidification of the cell culture medium on control samples with peak responsivity at 557 nm. In the visible region with phenol red media, peak absorbance values with a different number of cells at the wavelengths from 556 nm to 559 nm were identified related to absorbance of colour in the media. However, the absorbance spectra do not produce any noticeable peak that provides information on color in the visible region without phenol red media due to the colourless nature of the medium used for the cell culture. It was found that wavelengths between 966 nm and 985 nm have been identified to be highly related to water absorbance in the NIR region. The absorbance of cells slightly increased for each increment in the number of cells for all cell lines, highly attributed to light scattering by the cells. Spectral signatures for the examined cells were computed from linear regression (i.e. generated from the

relationship between absorbance from 400 to 1100 nm and the number of cells) parameters i.e. coefficient of determination, R^2 , and slope (responsivity). The pattern of spectral signature for the cells significantly increases the diverse characteristics between L929, HeLa, and DU145 cells. Multiple linear regressions (MLR) analysis was used to generate an algorithm to quantify cancer cells by using Minitab 18 Software. The best combination of a few best wavelengths of each cell has been identified to develop a spectroscopic algorithm with high R^2 and lowest root mean square of error, RMSE. The best measurement accuracy with $R^2 = 99.89\%$, $R^2 = 99.68\%$ and $R^2 = 99.63\%$ was produced with RMSE = 3390 cells, RMSE = 5277 cells and RMSE = 5647 cells for L929, DU145 and HeLa cells respectively for media with phenol red while media without phenol red for L929, DU145 and HeLa cells produced $R^2 = 99.94\%$, $R^2 = 99.91\%$ and $R^2 = 99.44\%$ with RMSE = 1860 cells, RMSE = 2754 cells and RMSE = 6938 cells respectively. The high measurement accuracy of the cells with a coefficient of determination above 0.99 was obtained from quantitative analysis for all types of cells. This study has proved that a wide range of spectrum range of VIS-NIR absorbance spectroscopy can be performed to differentiate between normal and cancerous cells which has potential as a cancer spectroscopic biomarker and as a tool for quantitative measurement of cells.

CHAPTER 1

INTRODUCTION

1.1 Research Background

Cancer is one of the major leading diseases that cause death in Malaysia and the second leading cause of death globally. According to GLOBOCAN 2018 database, lung cancer (18.4%), colorectal cancer (9.2%), stomach cancer (8.2%), liver (8.2%), and breast cancer (6.6%) are the main types of cancer cause of death in 2018. The main types of cancer are different from gender. The most common cancers and the leading cause of cancer death among males are lung cancer (14.5%), prostate cancer (13.5%), colorectal cancer (10.9%), stomach cancer (7.2%), and liver cancer (6.3%) for incidence while lung cancer (22.0%), liver cancer (10.2%), stomach cancer (9.5%), colorectal cancer (9.0%), and prostate cancer (6.7%) for mortality. Among females, the most common cancers and the leading cause of cancer death are breast cancer (24.2%), colorectal cancer (9.5%), lung cancer (8.4%), cervical cancer (6.6%), and thyroid cancer (5.1%) for incidence while breast cancer (15.0%), lung cancer (13.8%), colorectal cancer (9.5%), cervical cancer (7.5%), and stomach cancer (6.5%) for mortality (World Health Organization, 2018). The reasons for the unavoidable high percentages of incidence and mortality because of limited or non-existent resources, diagnosis, and treatment of cancer. Cancer can be treated if diagnosed at an early stage but if conditions of cancer are enhanced and spread already, a chance of surviving is mostly likely to decrease due to more difficult accurate diagnosis and effective treatment. All this can be prevented if cancer were diagnosed and treated early and rise the probability of the chance of 30-50 percentage if treated with the correct knowledge,

right prevention, and suitable strategies (Bray et al., 2018) (World Health Organization, 2018).

The most common diagnostic tests for cancer include imaging techniques for example magnetic resonance imaging (MRI), computed tomography (CT) scan, positron emission tomography (PET) scan, X-rays, ultrasound, and mammography. Other tests are used for more specific cancer such as endoscopic techniques (colonoscopy, sigmoidoscopy, and upper endoscopy), biopsy, tumor markers (carcinoembryonic antigen, CEA and prostate-specific antigen, PSA), digital rectal examination (DRE), and Pap test. Also, a simple review of health history, physical examination, laboratory tests such as blood and urine, and a genetic test is utilized for screening. The diagnostic result provides morphology and functional information to identify cancer and cancer stages to increase the chances of treated successfully and reduce the probability of death (Kondepoti et al., 2008) (Bethesda, 2002) (Cancer Treatment Centers of America, 2018).

Over the recent decades, optical spectroscopy has been employed in broad and diversified applications such as in the food industry and agriculture, polymer industry, arts, industrial, forensic, chemical, medical, and pharmaceutical. The application of optical spectroscopic methods in the diagnosis of cancer has been an intriguing interest during the past decades. The principle of optical spectroscopy based on the nature of the interaction between light and the object and usually classified as absorption, emission, elastic scattering (reflection), and inelastic scattering in examines the properties of physical objects (Yang, 2016). Application of spectroscopy has been agreed as a sensitive, non-destructive, and specific analytical method with a high perspective in various fields of research such as biomedical and cancer diagnosis with

a specific type of cancer (Bellisola & Sorio, 2012). Optical spectroscopy advanced largely in applications of many fields and areas due to quick data acquisition, high sensitivity, and reproducibility techniques (Janssens, 2003). Furthermore, optical technologies have many significant advantages over imaging techniques including fMRI, CT, or PET such as simple, non-invasive, fast, portable, and inexpensive methods for diagnosing cancer (Yu, 2012). Also, the medical application of optical spectroscopy could differentiate types of tissue based on the quality and ability of a tissue detection from specific range wavelength. With these advantages, optical spectroscopy has become a promising optical measurement technique for cancer diagnosis to distinguish between normal and cancerous tissues and cells (Evers et al., 2012).

1.2 The Fundamental of Cancer

Cancer is a disease that can be found throughout the trillion cells of the human body. The medical term for cancer is malignant tumours and neoplasm. Normally, cells have their own rule of cell division and follow the signal to grow, divide, and differentiate into a new cell or die in an orderly way. However, cancer cells disregard this order and become abnormal cells that grow and proliferate uncontrollably. These phenomena involve changes or mutations in the cell genome called deoxyribonucleic acid (DNA) mutations that produce a protein that disturbs the way of cell function. Cancer cells start to divide without stopping, unnecessary new cells are formed, damaged cells are survived, cells divided without stopping and spread into the surrounding tissue to another organ in the body called metastasizing and metastases are the major cause of 90% of cancer-related deaths. Figure 1.1 illustrates abnormal cell expansion from a single abnormal cell that leads to a mass of abnormal cells called

tumour after a few stages of mutation (National Cancer Institute, 2015) (Hejmadi, 2010). A tumour can be malignant or benign which is malignant can grow and spread to other parts of the human body while the tumor that can grow but will not spread is called benign (Bethesda, 2002). Basically, all mammalian cells have a similar molecular network that controls cell proliferation, differentiation, and cell death. Under those circumstances, research of cancer can be done in many ways includes using animal cells to study human cells in vitro (National Cancer Institute, 2015) (Hejmadi, 2010).

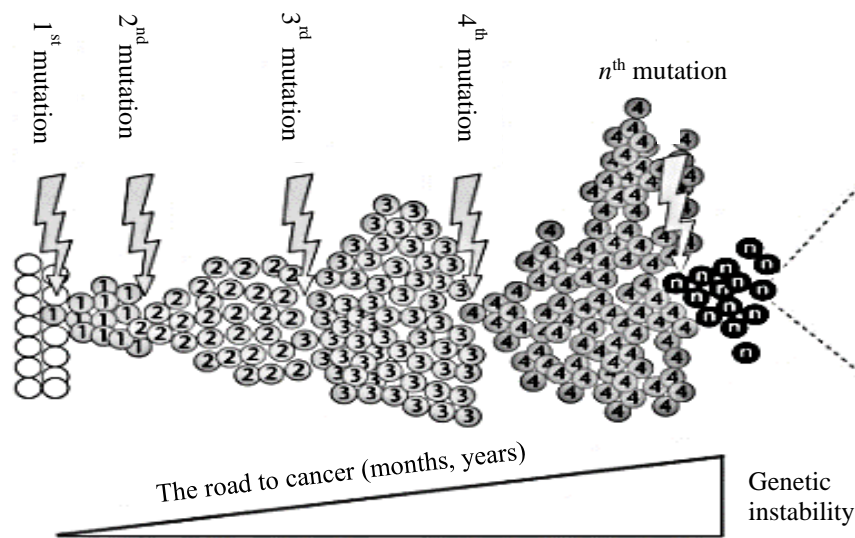


Figure 1.1 Abnormal cell expansion (Nejmadi, 2010)

1.2.1 Cervical Cancer

Cervical cancer is the fourth most commonly diagnosed cancer and the fourth leading cause of cancer deaths among women worldwide in 2018. Lately, rapid rises in premature cervical cancer deaths in the countries without the implementation of an effective screening program. Cervical cancer is the third in females and seven places in Malaysia (World Health Organization^b, 2019). Malaysian National Cancer Registry Report 2007 to 2011 stated breast (32.1%), colorectal (10.7%), cervix uteri (7.7%), ovary (6.1%) and lung (5.6%) cancers were the five most common cancers among

female and cancer of the cervix uteri was the third most common cancer in females and seventh in overall (Ab Manan et al., 2016). The incidence and mortality rates in Malaysia have failed to decrease mainly because of knowledge and behaviour among women in addition to Pap smear issues as a screening test and high-risk human papillomavirus (HPV) infection controversy (Zaridah, 2014).

Cervical cancer is a type of cancer that occurs in a woman's genital organ called the cervix and part of the woman's reproductive system. The cervix location is in the entrance to the uterus womb from the vagina. The important functions of the cervix are to help the process of pregnancy, childbirth, menstrual, and intercourse. The normal cell lining (squamous and glandular cells) in the cervix transform into cancerous after going through a series of changes over the years. Figure 1.2 illustrates the normal cell and different stages of cervical cancer. The cervical cancer stage ranges from less spread and lower stages I (1) through more advanced cancer, IV (Bethesda, 2002). The two main types of cervical cancer are known as squamous cell carcinoma and adenocarcinoma. Adenocarcinoma indicates to glandular cells that are cancerous was used for this research study. Scientific evidence has found that screening women for human papillomavirus (HPV) is the virus that causes cervical cancer (Cancer Council NSW, 2017) (National Cancer Institute, 2019). Figure 1.3 shows the multiphoton fluorescence image of HeLa cells. There are 3 major differences between normal and HeLa cells. First, the difference between normal cells and HeLa cells is most visible at the chromosomes in which the normal cell contains 46 chromosomes whereas HeLa cells contain 76 to 80 total chromosomes. Second, HeLa cells grow easily, rapidly, and unusually fast in 24 hours which is ideal for large scale testing. Lastly, HeLa cells are continuous to divide the cells due to the overactive telomerase (Faussadier, 2017).

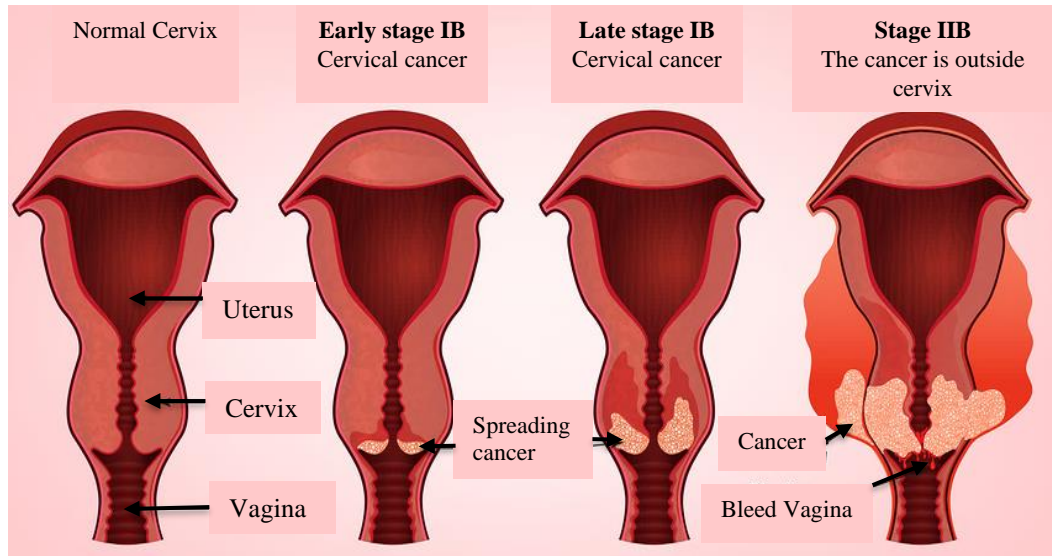


Figure 1.2 Normal cell and different stages of cervical cancer cells (Schilling, 2018).

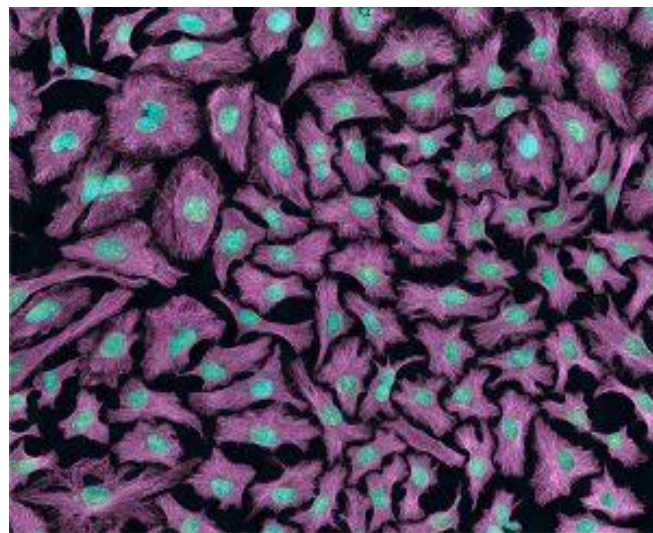


Figure 1.3 Multiphoton fluorescence image of HeLa cells with cytoskeletal microtubules (magenta) and DNA (cyan) using Nikon RTS2000MP custom laser scanning microscope (Image by National Institutes of Health (NIH)).

Screening is the process of searching for cancer or precancerous changes to an asymptomatic target population and act as a precursor of the disease. For several decades, the Pap test known as Pap smear has been used as a screening test for cervical cancer. Other screening tests such as HPV testing, visual inspection with acetic acid (VIA) and liquid-based cytology (LBC) are used but not all the test is a suitable

screening programme for the disease. Usually, the screening programme is influenced by many different factors and varied or modified the screening test to apply in a certain country such as cost, availability, tool, equipment, and human resources. Therefore, a diagnostic test is highly regarded for the affirmative and definitive diagnosis of cancer detection. The most common tests are colposcopy, biopsy, and endocervical curettage (ECC). It produces significant results despite that, diagnostic tests need training, a high level of knowledge, more resources, and good management (World Health Organisation, 2014). Up to the present time, there are many diagnostic tests and equipment that have been studied to accomplish high performance of cervical cancer detection.

1.2.2 Prostate Cancer

Generally, prostate cancer is a type of cancer in the genital part of man that is the second most common cancer in men, the fifth leading cause of cancer deaths, and third worldwide if both genders combined in 2018. Cancer incidence is influenced by the diagnosis of latent cancers by PSA testing. Mortality cases in many countries have been reducing attributed to earlier diagnosis (Bray et al., 2018). Malaysian National Cancer Registry Report 2007 to 2011 stated the colorectal (16.3%), lung (15.8%), nasopharynx (8.1%), lymphoma (6.8%) and prostate (6.7%) cancers are the five most common cancers among males in Malaysia. According to the World Health Organization, prostate cancer is the third in males and fifth places in Malaysia in 2018. (World Health Organization^c, 2019). Tun Firzara & Ng (2016) mentioned the increase in incidence rate in Malaysia related to the age and prostate cancer screening rate becoming more widely available in the country.

The prostate gland is a reproductive organ of a male that located in front of the rectum surrounds the urethra, and between the bladder and the penis. The main

function is to secrete a seminal fluid that aids sperm in nourishment and transportation. Prostate cancer is when normal cells in the prostate change and grow uncontrollably forming a mass called tumor. Figure 1.4 shows the difference between normal prostate and prostate cancer. A normal prostate has no problem with the flow of urine unlike prostate cancer has obstruction caused by enlarged prostate cancer press on the bladder and urethra leads to urinary tract blockage (Mandal, 2018). The types of prostate cancer include adenocarcinomas, sarcomas, neuroendocrine tumors, small cell carcinoma, transitional cell carcinoma, squamous cell carcinoma, and sarcomatoid carcinoma (Martin et al., 2007). Adenocarcinomas type was chosen for this prostate cancer research as one of the biological samples because more than 95% of prostate cancers are from this type of cancer (Mottet et al., 2015).

DU145 cells had a normal nucleus, cytoplasm, and organelle morphology (Nie et al., 2016). Figure 1.5 shows the shape of DU145 cells with 100x magnifications (Carey et al., 2009). Normal prostate and prostate cancer cell lines fail to differentiate and form multicellular structures in the purely collagen-rich extracellular matrix. Prostate cancer is associated with a poor survival rate. The ability of cancer cells to evade apoptosis and exhibit limitless replication potential allows for the progression of cancer from a benign to a metastatic phenotype. DU145 cells are used as a classical example of late-stage prostate cancer and have moderate metastatic potential. The cell line is only weakly positive for acid phosphatase and exhibits very low DHT activity (Mahoney et al., 2014).

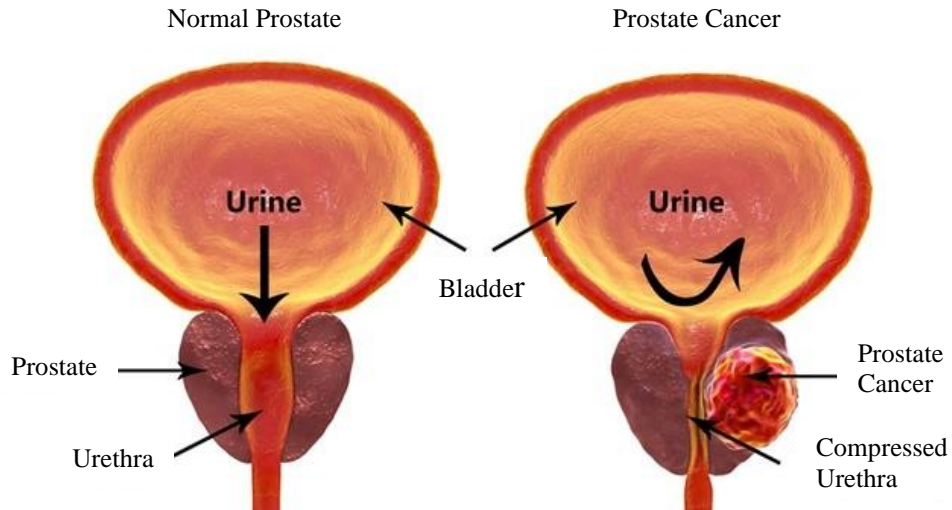


Figure 1.4 Illustration of normal prostate versus a prostate with a tumor prostate cancer. (Mandal, 2018).



Figure 1.5 Morphology of the DU145 cell lines in culture with 100x magnification. DU145 cells show a more mesenchymal morphology that is long and spindle-shaped (Carey et al., 2009).

Screening and early detection of cancer can reduce the chance of high complication and death. However, some prostate cancers have problematic characteristics that grow very slowly and almost without any symptoms or problems over the years. Afterwards, if cancer cannot be detected early, uncontrolled, and then unsuccessful treatment will lead to death. Prostate-specific antigen (PSA) is commonly used as a screening test and the death rate can be reduced by 20% but a high risk of overdiagnosis (Mottet et al., 2015). Besides, behaviour associated with screening

depends on the medical practitioner's decision-making to perform the PSA test and the accuracy was overestimated by them (Tun Firzara & Ng, 2016). There are many tests, tools, and health examinations up to the present time to detect prostate cancer emphasize the importance of screening for better treatment.

1.3 Skin Fibroblasts

Over the years, an animal being used to study the basic principles of life and to grasp a better understanding of the animal and human anatomy, physiology pharmacology, and pathology. In fact, a great number of animal models have been used for example rat, mouse, pig, primate, murine and porcine in experimental research to replace human skin (Lönnqvist, 2016) (Takeuchi et al., 2011). The most common animal models are the types of rodents such as a mouse, rat, and guinea pig for in vitro and in vivo experimental studies of skin permeabilities. The advantages of these species of animals that are small size, and it is simple to experiment with and produced a significant result in the study of the gene product (Takeuchi et al., 2011) (Nyman, 2015). Animal biological models are the scientific methods of experimenting under controlled situations and mimicking biological conditions of human and animal diseases. Animal models contributed to the advancement in biological fields with scientific knowledge and provide life quality development such as new drugs and vaccines. It can be proven with 90% of Nobel Prize research in Physiology and Medicine, used animal experiments in their findings (Andersen, Winter, & Andersen, 2017). The model animal of a mouse has been used in this study regardless of some differences in skin structures and characteristics and has varied with different species of animals.

Mouse skin fibroblast was chosen as a control cell for this research study as a normal cell to be compared with cancerous cells. Before that, the differences between mouse and human skin as and tabulated in Table 1.1 (Pasparakis et al., 2014) (Lawlor & Kaur, 2015). Fibroblasts are significant cells of the connective tissue that secrete collagen proteins and extracellular matrix and provide the structural framework in many tissues (Khan & Gasser, 2016). The most abundant cells of fibroblast are found in the loose connective tissue and in charge as precursors. The ability of fibroblast to cultivate in vitro easily due to minimum demand of growth specification compared to other human cell types have assisted in a greater understanding of the biology of these cells as well as other cells which used these cells as control cells (Badawy et al., 2005).

Table 1.1 Differentiate between mouse skin and human skin (Pasparakis et al., 2014) (Lawlor & Kaur, 2015).

Skin Structure	Mouse	Human
Hair follicle	- Densely packed - Higher density	-Larger areas of interfollicular skin with sparse - Lower density
Epidermis	- Thin - Langerhans cells and CD8 ⁺ T cells - V γ 5 ⁺ dendritic epidermal T cells (DETCs)	- Thick - Langerhans cells and CD8 ⁺ T cells
Epidermis layer Characteristics	Fewer layers (3 layers) - Mostly absents of rete ridges and dermal papillae	More layers (6-10 layers) - The undulating pattern of rete ridges - Alternating dermal papillae,
Dermis	- Thin -Macrophages, mast cells, conventional $\alpha\beta$ T cells and innate lymphoid cells, ILC - $\gamma\delta$ T cells to skin immune surveillance and interleukin-17 production	- Thick - Macrophages, mast cells, conventional $\alpha\beta$ T cells and innate lymphoid cells, ILC
Features	- Psoriasis has not been observed in animals	-Prominent in psoriasis and correlates with elongation of the dermal papillae known as papillomatosis.

1.4 Cell Culture and Cell Culture Media

Cell culture is the process of cell removal from an animal or plant includes sustaining cells of multi-cellular organisms outside of their original (in situ) body and their next growth under convenient artificial environments. A cell is important as it is the basic unit of life and a popular tool of experimentation in biology research to study growth factor, functional enzyme, production of the vaccine, and a variety of other uses in the medical field and cell culture is the essential process to obtained those purposed (Praveen & Mounika, 2017). Cancer cell lines have been used for this research to study normal and cancer cells. There are three different techniques to remove the cell from tissue includes the primary explant technique which is derived from a cell line or cell strain or mechanical and enzymatic disaggregation directly from tissue removal as shown in Figure 1.6. Figure 1.7 shows the step of the animal organ cell culture of normal and cancer cells to produce cell lines by using the enzymatic disaggregation method. Cell lines derived from primary cultures have a limited life span and are linked to passage numbers. A passage number is a total of how many times a cell line has been sub-cultured specifically (Invitrogen, 2010).

Application of cell culture has been implemented in many fields such as in protein therapeutics, vaccines, and cancer research which has been used in this study. Furthermore, cell culture also equally important in applications of model system, virology, toxicity testing, genetically engineered protein, replacement tissue or organ, genetic counselling, gene therapy, drug screening, and development (Roy et al., 2019) (Kumar, 2015). Cell culture also can be used to convert normal cells into cancer cells by methods including radiation, chemicals, and viruses. These cells can then be used to study cancer more closely and to test potential new treatments (Applied Biological Materials Inc., 2015).

Phenol red is a common pH indicator that is available within most commercial cell culture media to monitor the cellular environment. Phenol red changes color depending on the pH level (Magnusson et al., 2013). Phenol red has been used in various colorimetric applications, such as the examination of freshwater pH (Lai et al., 2016), the diagnosis of filarial infection (Poole et al., 2017), and the measurement of hydrogen peroxide produced by cells in culture (Pick & Keisari, 1980) and carbon dioxide pressure in carbonated liquids (Mills & Skinner, 2011). Phenol red has also been applied in assisting biopsy procedures to determine *Helicobacter pylori*-infected areas for patients with early gastric cancers (Iseki et al., 1998).

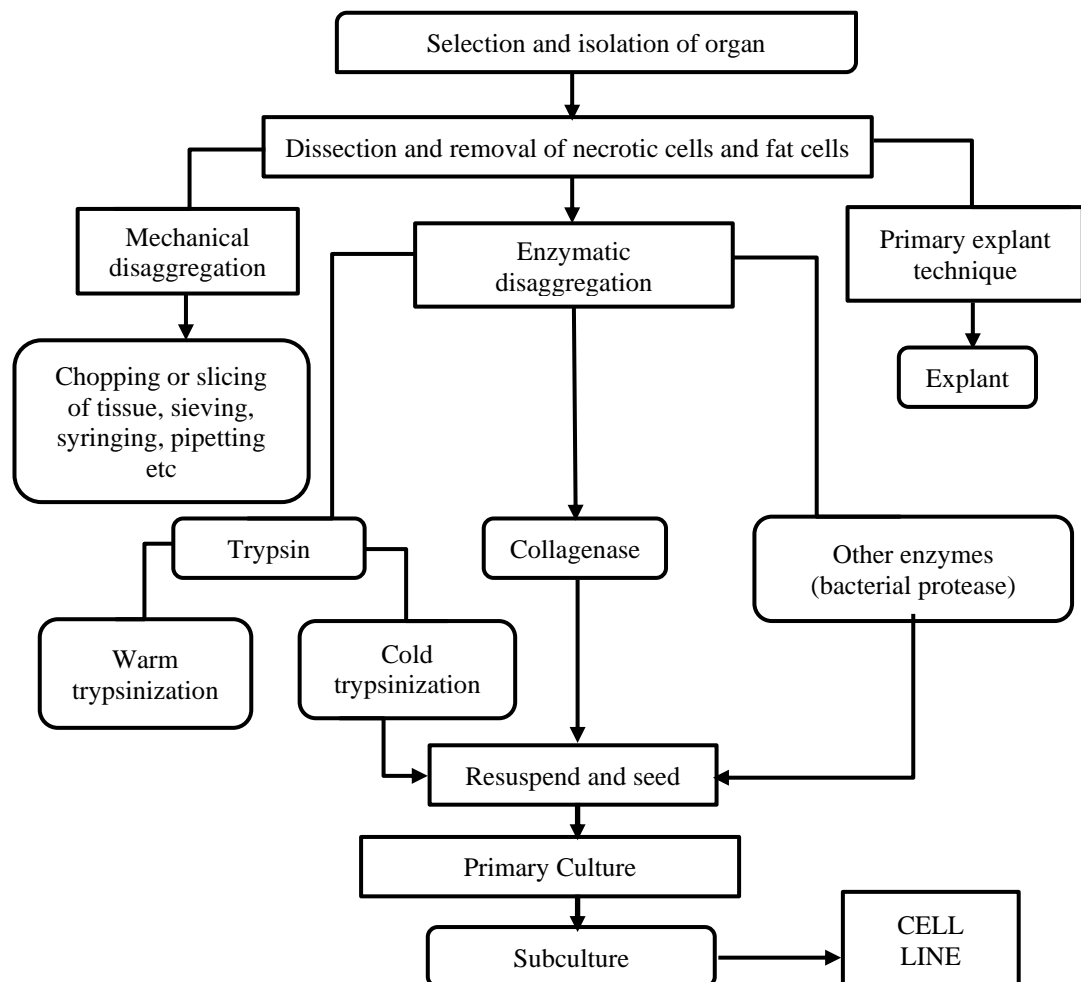


Figure 1.6 Different techniques used for primary culture (Jha, 2015).

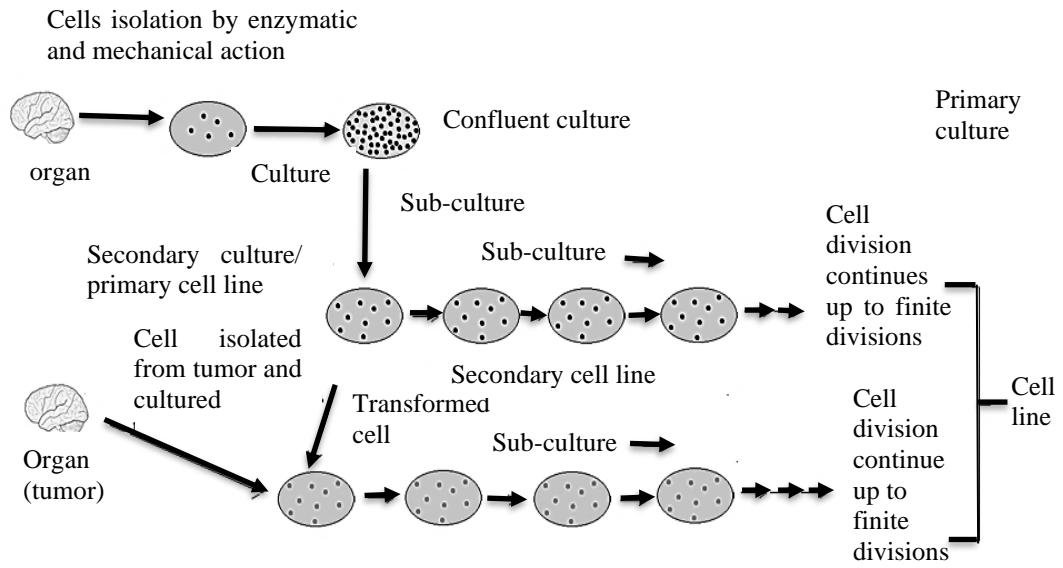


Figure 1.7 Animal cell culture to produce a cell line (Khanal, 2017).

Morphology cells in culture can be divided into three basic categories based on their shape and appearance as shown in Figure 1.8. In Figure 1.8 (a), morphology cells are called fibroblastic or fibroblast-like cells. Cells are bipolar (multipolar), elongated shapes, and grow attached to a substrate. Figure 1.8 (b) shows epithelial-like cells that polygonal shapes, regular dimension and grow attached to a substrate in distinct patches. Lastly, lymphoblast-like cells are spherical shapes and grown in suspension without attaching to a surface as shown in Figure 1.8 (c) (Invitrogen, 2010).

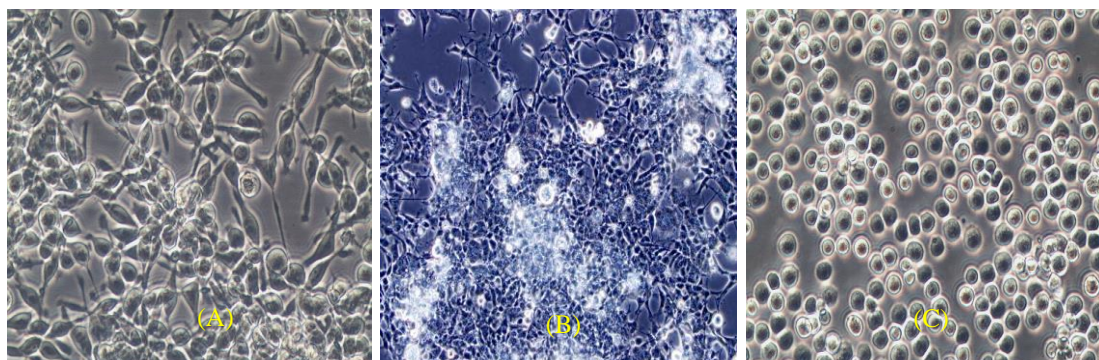


Figure 1.8 Basic categories of morphology cells in cell culture based on shape and appearance (A) fibroblastic, (B) epithelial, and (C) lymphoblast. The images were obtained using 20x magnification (Invitrogen, 2010).

Cell culture media is essential for cell culture and affects the growth factor contains amino acids, inorganic salts, and vitamins. A specific type of media is required for different cell lines. In this study, two sets of media were used for each cell line, with and without phenol red complete medium. Generally, phenol red is added to cell culture media as a pH indicator for monitoring and maintaining cell viability. The visible color varies from yellow (pH 6.4) to red (pH 8) by visual inspection in culture tools and qualified for a non-invasive optical test in cell culture (Lopez-Martinez et al., 2010). Nonetheless, the similarity of structure between molecules may lead to interference and affect the results (de Faria et al., 2016). Recently, the important of microfluidics cell culturing in biological and biomedical research have been performed for methods of evaluating condition such as pH inside a microfluidic system. Cells have the ability to rapidly change the environment within a microchannel. For that reason, the culture parameters are needed to be controlled (Lopez-Martinez et al., 2010).

1.5 The Fundamental of Optical Spectroscopy

Spectroscopy is the study of the interaction between light and matter as a function of wavelength. Spectrometry is a method of studying and measuring a specific spectrum used for the spectroscopic analysis of sample materials and the spectrometer is the instrument that carries out the measurements (Foundation, 2009). In the spectroscopy analysis, the two interactions of light with atom and molecule can be applied to identify the specific wavelength and to measure the total amount of light absorbed or emitted at a specific wavelength (Ocean Optics, 2017). There are three types of spectroscopy includes atomic and molecular spectroscopy. Second, classify based on the property of either absorption or emission which is absorption

spectroscopy includes UV-VIS spectroscopy, infrared spectroscopy, nuclear magnetic resonance (NMR), atomic absorption spectroscopy while emission spectroscopy which is fluorimetry and flame photometry. Lastly, based on electronic or magnetic properties of the compound which have both electronic and magnetic properties for examples of electronic spectroscopy (colorimetry, UV-spectroscopy, IR, fluorimetry, etc) and magnetic spectroscopy examples include nuclear magnetic resonance spectroscopy (NMR) and electron spin resonance spectroscopy (ESR) (Ranga.nr, 2019). Globally, spectroscopy techniques are used in the science of chemistry, biology, engineering, and physics. This research study will focus on the spectroscopic analysis of the cell's absorbance spectra to identify and quantify the cancerous cells.

1.5.1 Overview of VIS-NIR Spectroscopy

Optical spectroscopy is the methods that utilize the interaction of ultraviolet (UV), visible, and infrared (IR) radiation with the matter by using optical material to disperse and focus the radiation. This study focuses on absorbance visible and near-infrared (VIS-NIR) optical spectroscopy. As light passes through matter, the number of photons decreased as some of it is absorbed called absorbance, and the absorbance spectrum is a plot of absorbance as a function of the photon energy or wavelength. The spectrum can identify and calculate the amount of the compound. The radiation intensity at a significant wavelength is attenuated called absorption and absorption spectroscopy is to measure the light is absorbed in each wavelength. Absorbance is an alternative method for describing the attenuation of electromagnetic radiation (Harvey, 2009). As shown in the complete electromagnetic spectrum in Figure 1.9, light in the visible and NIR region only a small region of the entire spectrum of electromagnetic radiation. The visible and NIR region is a benefit for analysing samples non-destructively.

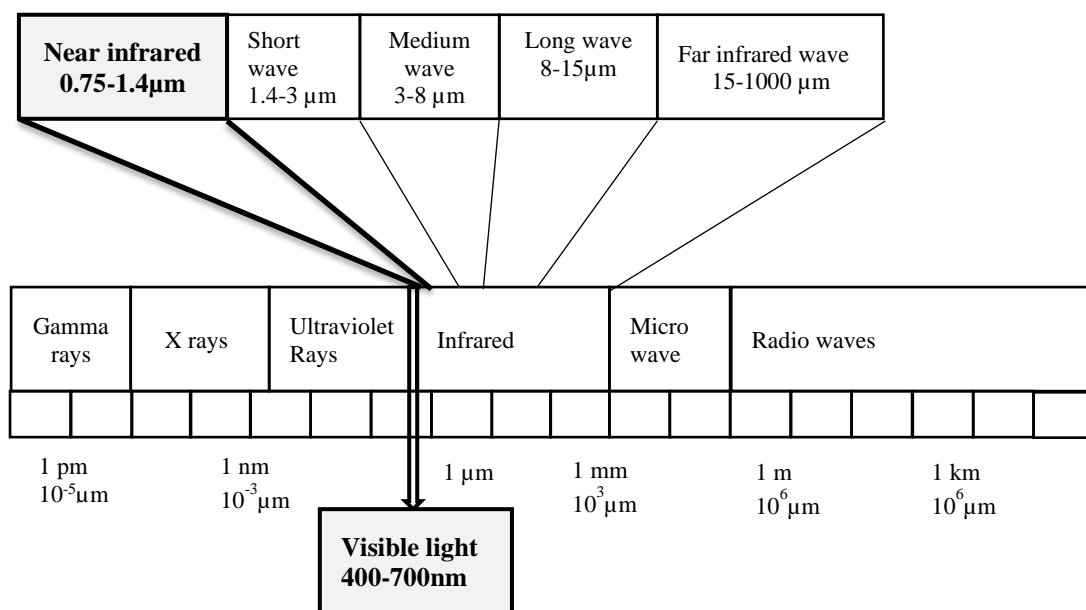


Figure 1.9 The electromagnetic spectrum describes the various types of electromagnetic energy based on the wavelength (Protherm, 2005).

In the visible range, the spectrum study of absorption or emission as many atoms emit or absorb visible light. It is a very popular indicator of color distinguisher. The NIR range provides greater wavelength and penetration depth into the samples (Foundation, 2009). It is also the main tool to study the organic compound. There is the vibration of bonds between carbon, hydrogen, oxygen, and nitrogen atoms that predominate in organic compounds which are used to identify the compound with characteristic features and functional group (Ocean Optics, 2017). Therefore, the application of NIR spectroscopy is used in many fields such as rapid grain analysis medical diagnosis pharmaceuticals/medicines, biotechnology, food analysis, and chemical imaging or hyperspectral imaging of intact organisms, plastics, textiles, insect detection, and so on (Foundation, 2009).

1.5.2 The Interaction of Light with Matter

Electromagnetic radiations are classified into two categories which are ionizing radiation (far ultraviolet, x-ray photon, gamma photon, and particle radiation) and another one is non-ionizing radiation (radio waves, microwaves, visible, infrared, and near-ultraviolet). Electromagnetic radiation in the electromagnetic spectrum as shown in Figure 1.9 is emitted when an atom moves from an excited state to a state of lower energy and is absorbed when an atom moves from a lower state to a higher state. Particle-wave dualism is the properties of matter which has both particle and wave function. The basic interactions of light with matter include reflection which the light will return from the surface, diffraction with light will diverge from rectilinear propagation, and alignment of the electric vectors to other orientation known as polarization. The emission of light from the return of a molecule from a singlet excited state to the ground state and loss the energy called fluorescence, resonance absorption is the energy of the incident photon is just equal to the first excited state of the atom, elastic scattering or Rayleigh scattering is the incoming and outgoing photons have the same energy and inelastic scattering or Raman scattering is the energy of the scattered photon is less than the incident photon. Additionally, the light-matter interaction also involves the photoelectric effect, Compton scattering, and stimulated emission. Upon these interactions, the characterization of a particle can be done as they absorb or emit electromagnetic radiation with spectroscopic methods. Furthermore, the molecular structure, quantitative, and qualitative both inorganic and organic compounds can be acquired with spectroscopy methods (Riepe, 2001).

1.5.3 Absorbance and Concentration: The Beer-Lambert Law

The linear relationship between concentration absorbance and concentration is called the Beer-Lambert law. The light passes through a thin layer of sample thickness

(dx) is decreased in its power (dP) which proportional to the sample's thickness and analyte's concentration of the samples (C). P is the power incident on the thin layer of the sample. The concentration using molarity, a is the absorptivity with units of $\text{cm}^{-1} \text{conc}^{-1}$ is changed with the molar absorptivity, ϵ ($\text{cm}^{-1} \text{M}^{-1}$). The absorptivity and molar absorptivity are proportional to the probability that the analyte absorbs a photon of a given energy. For that reason, both values of a and ϵ depend on the wavelength of the absorbed photon (Harvey, 2009). Therefore, the equations can be written as:

$$-\frac{dP}{P} = \alpha C dx \quad (1.1)$$

$$A = \alpha C d \quad (1.2)$$

$$A = \epsilon C d \quad (1.3)$$

Where,

A = Absorbance

α = Proportionality constant

ϵ = Molar absorptivity

C = Concentration of the absorbing samples

d = Samples pathlength

1.5.4 Optical Spectroscopy in Cancer Diagnosis

The understanding of the urgent importance of early diagnosis of cancer has led to many common diagnostic tests such as x-ray, magnetic resonance imaging

(MRI), computed tomography (CT), single-photon emission computed tomography (SPECT), positron emission tomography (PET) ultrasound and endoscopy have been applied to diagnose many types of cancer tissues. Other diagnostic tests such as biopsy and histopathological analysis of the tissue also are regarded as an adequate method of cancer diagnostic (Frangioni, 2008). However, these methods are invasive and overdiagnosis may develop radiation-induced cancer (Taroni et al., 2017) (Messadi et al., 2014) (Moy et al., 2016). The purpose of cancer detection is to prevent death from cancer by reducing the incidence of cancer disease and thus implementing effective treatment. Tests are associated with advantages, limitations, and harms, and all these must be carefully thought about to provide effective cancer detection. The advantages of early detection reduce the risk of being diagnosed with advanced cancer. Some limitations and harms include false test results, overdiagnosis, and might even have injury and death associated with the diagnostic evaluations (Wender et al., 2019).

To optimize the diagnostic need, the optical spectroscopy technique currently has popularly emerged as a non-invasive alternative to various conventional measurement techniques and cancer diagnostic in the medical field and utilized in the past decades. The application of optical spectroscopy has many beneficial include non-invasive methods, cost-effective, portable, easy to use, rapid measurement, and non-ionizing which could fulfil the requirement for conventional cancer diagnosis tools and methods (Edwards et al., 2017) (Kallaway et al., 2013). Spectroscopy can be used to perform diagnosis complications of in situ cancer detection due to significant living tissue variation in blood content, water content, collagen content, and fiber development from person to person, site to site, and time to time on the same site (Jacques, 2013). Spectroscopy measurement provides information about absorption and scattering on the biochemical composition and microscopic structure of the tissue

(Taroni et al, 2017) (Sokolov, 2002). Furthermore, optical characteristics may act as a biomarker to differentiate between cancerous and normal tissue claimed by Solano et al (2012) in their research study. Therefore, there is a must in exploring optical spectroscopy to comprehensively characterize and provided spectral signatures of cancer cells to analyse the spectral response compared to the complexity of cancer in the form of tissue. Additionally, optical spectroscopy can be applied in the measurement of a small number of cells which is important to be specifically quantified for cancer biomarkers in early cancer detection. In this study, the assessment of cancer detection for quantification is taken with optical spectroscopy and focused on early cancer detection.

1.6 Problem Statement of the Research

The problem statements cover an area of social concern and addressing sustainable development goals and also research gaps in cancer detection.

1.6.1 Social Concern and Addressing Sustainable Development Goals

Today, cancer as a second leading cause of death worldwide causes so much attention with rapidly increasing in the number of incidence and mortality globally with 1 in 6 deaths is due to cancer. In 2018, it is calculated around 18.1 million new cancer cases and 9.6 million deaths occurred worldwide with only 14.1 million (incidence) and 8.2 million (mortality) in 2012 and predicted may rise to 24 million in 2035. Since the 20th century, early diagnosis has been recognized as one of the most important and necessary parts of reducing cancer mortality to provide effective treatment before cancer spread regionally or to the other organ. This research is in-line with the United Nation Sustainable Development Goal (Goal #3) in ensuring healthy lives and promote well-being for all of all ages. This research is also in harmony with

Ministry of Health Malaysia's National Strategic Plan for Cancer Control Programme 2016-2020, Section 8.2.3, Page 32 that highlighted its objective to improve the accuracy, efficiency, accessibility, and timeliness of cancer diagnosis (Ministry of Health Malaysia. National Strategic Plan for Cancer Control Programme 2016-2020, 2017).

1.6.2 Research Gaps in Cancer Detection

The identification of cancer border is critical especially during surgery to ensure complete removal of diseased cells. In current practice, the removal of tissue during surgery is conducted with 1 to 2 cm of safety margin. However, for cosmetic reasons, such a large margin is undesirable, especially on the face and neck. Even worse if there are cancer cells left behind that require a repeat surgery (Meng et al., 2016). There is a significant variation in blood content, water content, collagen content, and fiber development within living tissue from person to person, site to site, and even from time to time on the same site (Jacques, 2013). This factor significantly raised the complexity of clinical in situ cancer detection. Furthermore, the interface between cancer and normal tissue is difficult to be determined, especially after cancer cell invasion into normal tissue (Jermyn et al., 2017). Hence, there is a need to comprehensively characterized and established spectroscopy signatures of cancer at the level of the cells to better understand the spectral response obtained rather than a highly complicated cancer in the form of tissue. Moreover, several structural and functional cellular traits can be understood through the experimental determination of the physical properties of living cells (Neto et al., 2006). There is also a great need to accurately quantify predictive biomarkers for cancers (Brown et al., 2009), especially in the measurement of a small number of cells in early cancer detection (Solano et al., 2012). Capability to acquire quantitative characteristics of cells directly from the living

system (in situ) is important in monitoring morphological and physiological changes particularly in the precancerous or cancerous state (Backman et al., 1999). Disease diagnosis via analysis on a few cells is always preferable compared to a more invasive technique such as surgical (tissue) biopsy (Bassan et al., 2010). This highlights the essential advantage of cytopathology compared to tissue biopsy. Cytology method such as fine-needle aspiration offers cost-effective, simple, accurate and a safe procedure compared to tissue biopsy (Al-Abbadi, 2011). However, the analysis of cells visually using an optical microscope is subjective and time-consuming though conducted by highly trained cytopathologist (Bassan et al., 2010) (Clemens et al., 2014). The cytopathologist is required to positively classify and diagnose a small number of cells within a sample containing about 10,000 cells. The cells may display delicate morphological alterations in the early stages of dysplasia (Schubert et al., 2010). For the case of pap smear, the sensitivity and specificity of the diagnosis method are relying on several possible subjective practices such as the skill of the observer in identifying a variety of cellular abnormalities, poor sampling, low number of abnormal cells in the sample, and existence of biological contaminants in the sample (Wood et al., 2014). Immunohistochemical stains on the sample assist in the diagnosis procedure but still subject to subjective assessment (Bassan et al., 2010). Therefore, it is crucial to develop a new diagnostic method that can aid cytopathologists to perform cytological examinations for the early detection of disease. The method ought to be rapid through minimal sample preparation, relatively low cost, and nondestructive. Cellular diagnosis should utilize a more objective analysis (Clemens et al., 2014).

1.7 Aim and Objectives

The aim and objectives of the entire research to be achieved at the end of this study.

1.7.1 Aim

To date, though spectroscopy techniques have been widely used to diagnose various types of cancer tissues, information on optical spectroscopy properties of cancer cells is not extensively available, especially for the quantitative evaluation of cells. The objective of this research is to examine quantitatively and to develop a spectral signature for cervical (HeLa) and prostate (DU145) cancer cells through visible and near-infrared (VIS–NIR) absorbance spectroscopy technique. The experiment on mouse skin fibroblast (L929) was also conducted as a reference. Human cervix adenocarcinoma (HeLa) and human prostate carcinoma (DU145) are among the most commonly used cancer cells and often used together in cytotoxicity (Ma et al., 2018)(Ibrahim et al., 2019), anticancer (Xu et al., 2019)(Diao et al., 2019), antiproliferative (Ndung’u et al., 2018)(Rayla et al., 2018) and diagnosis (Ko et al., 2011) studies. Mouse fibroblast cell line (L929) on the other hand are internationally recognized cells that are routinely used in in vitro cytotoxicity studies (Cochrane et al., 2003) and have been used as a control or normal health counterpart to cancer cells in cytotoxicity (Mousavi et al., 2011) and diagnosis assessment (Chen^c et al., 2015). Besides, L929 cells can be easily cultured and reproducible (Swain et al., 2014). The focus of this research primarily is to examine the accuracy of VIS–NIR spectroscopy to quantify the concentration of different types of cells in cultured cell lines and the potential of the developed spectral signature as a cancer biomarker. The optical or spectroscopic biomarker for cancer cells has promising application and can set as a